XFEL.EU TN-2014-001-01

TECHNICAL NOTE

Design Report / Production Readiness Report

The Undulator Commissioning Spectrometer for the European XFEL

December 2013

W. Freund

for the X-Ray Photon Diagnostics group (WP74)

at European XFEL

European X-Ray Free-Electron Laser Facility GmbH

Albert-Einstein-Ring 19

22761 Hamburg

Germany

Contents

Introduction

At the European XFEL, two hard X-ray self-amplified spontaneous emission (SASE) undulators and one soft X-ray SASE undulator will be used for producing high brightness laser radiation. The hard X-ray undulators SASE1 and SASE2 will consist of 35 undulator segments, each 5 m long, separated by 1.1 m long intersections for e-beam steering, focusing, and phase adaptation. For the soft X-ray undulator, the setup is similar but has less segments.

One prerequisite for achieving lasing is the tuning of the K-value of all undulator segments to a very high precision. This magnetic tuning of the undulators is done in the magnetic lab before the transport to the final position in the tunnels. When mounted in the tunnels, there is no possibility to measure the K-values directly by means of magnetic measurements. The undulator commissioning spectrometer, also known as the "K-monochromator" or "K-mono", will make it possible to measure the spontaneous radiation of the undulator segments for K-tuning and other diagnostic measurements (e.g. pointing and phase matching).

1 Project organization plan

The goal of this project is to develop and build up three spectrometers for the examination of the spontaneous radiation and the commissioning of the three SASE undulators.

1.1 Organization

This project is conducted by the X-Ray Photon Diagnostics Group (WP74):

- Scientific director:

  Serguei Molodtsov (serguei.molodtsov@xfel.eu)

- Work package leader:

  Jan Grünert (jan.gruenert@xfel.eu)

- Project leader:

  Wolfgang Freund, development and engineering (wolfgang.freund@xfel.eu)

- Imaging devices for the final versions:

  — Cigdem Ozkan (until October 2013)
  — Andreas Koch (from December 2013)

- Collaboration with Helmholtz-Zentrum Berlin (HZB) by means of a memorandum of understanding:

  — Calculations, simulations, and ray tracing
  — Tests at BESSY II

1.2 Project plan

The current project plan was shifted to allow further investigations of different commissioning methods. Some delay may also occur as the available work package human resources (engineering) are also needed for other projects (e.g. diamond detector and wavefront imager).

The given times include only rough estimates of the work of other work packages. For example, the DAQ and Control Systems group (WP76) has separate time schedules for the integration of the devices.

Furthermore, we have given the earliest possible milestone dates (Table 1). As the device is actually not needed before the accelerator is set to operation and the first undulator is operated, the time schedule might be shifted due to priority changes within the work package.

Table 1: *Milestones and dates*

Milestone	**Date**
Conceptual design report (CDR)	9 December 2010 (meeting) April 2011 (final approval of amended documents)
Design Report	December 2013
Production Readiness Review	December 2013
Ready For Installation (RFI) SASE1	May 2014
RFI SASE2	October 2014 (see Section 1.5, “Final devices for tunnel installation”)
RFI SASE3	July 2014

1.3 Current status

As of this writing (December 2013), the following milestones have been met:

- Prototype (reduced setup, see below) has been built in a new lab at HERA South.

- Mechanical setup and the principle functions of the control system for motor control and camera readout have been tested.
- Proof of principle for single segment gap tuning was successfully completed at PETRA III (July 2012).
- Full version: Parts for cooling, second stage, and adjustment stage were purchased with a 3–4 month delay (DESY workshop order took 6 months). Assembly of the first full version started in November 2013.
- Critical parts for final versions were purchased. Example: Crystals for all monochromators were purchased from commercial vendor and are in house. (Production at HASYLAB crystal lab was not possible.)

1.3.1 Prototype

The first channel-cut crystal was manufactured in the crystal lab of HASYLAB and was characterized during a beamtime at BESSY II in February 2012.

In May–June 2012, one prototype of the K-mono was built. It was tested during two beamtimes at DORIS BW1 in June 2012 and at PETRA P01 in July 2012. The prototype was built up as a two-bounce version with imaging detection, consisting of a YAG:Ce screen with camera and a photodiode detector. For details, see Chapter 5, “Prototype tests”.

1.4 Calculations and simulations

Collaborations with the Simulation of Photon Fields group (WP72, led by Gianluca Geloni) and HZB (Alexei Erko, Franz Schäfers, and Jens Rehanek; Ref. [10]) have been established. Different scenarios are investigated.

The two main scenarios are:

- Quadrupole kick method (imaging of beam profile of two adjacent undulators)
- Single segment method (one undulator segment, photodiode detection, and energy scan: mono, beam, or gap)

1.5 Final devices for tunnel installation

The first prototype device will be used, after all modifications are made, as the final version for SASE1 (XTD2). As soon as the final versions are defined, the two remaining monochromators will be built. All parts for which the specifications are well defined will be ordered even before the PRR in order to achieve a lower price and better delivery schedule. This is the case for the channel-cut crystals, the rotational stages, the vacuum chambers, and some mechanical parts.

1.5.1 K-mono for SASE2

In tunnel XTD1, the photon beamline crosses the tunnel, and a collision of the photon beam components with the transport path must be solved. It is planned to take over the technical solution from the Tunnel Installation group (WP33) for a hanging support of the e-beam components in XTD2, where the same problem appeared for the electron beamline, which crosses the tunnel. For details, see the minutes of the "Section Coordination Meeting XTD 1–5, XS 1–4, XSDU 1+2" and the "XFEL Photon Tunnel Coordination Meeting".

As at least the design of the vacuum chamber and the support frame of the SASE2 version is affected, the given RFI milestone is likely to shift.

2 High-level use cases

This section describes the basic purpose of the undulator commissioning spectrometer (K-mono) for the European XFEL facility.

2.1 System setup

The K-mono system consists of a crystal monochromator in Bragg geometry, a detection chamber downstream of the monochromator chamber, and a small upstream vacuum chamber with filter foils for energy calibration.

2.2 Purpose

The K-mono is designed for use with spontaneous radiation and selects a narrow bandwidth of the X-ray photon beam in order to tune the undulator segments. This process is called photon beam–based alignment (PBBA) and will minimize the difference in the undulator parameters K between undulator segments and optimize the phase between segments. The photon source could be a single segment, two adjacent segments, two distant segments, and up to all undulator segments at once. For single or few segments and to increase flux, pulse trains of spontaneous radiation could be used, while for an undulator configuration where lasing is possible, only single light pulses at 10 Hz (single pulse operation) are allowed. The design must be consistent to allow for imaging of the weak single segment spontaneous radiation and, on the other hand, to ensure the survival in free-electron laser (FEL) radiation in single pulse operation for FEL diagnostics. The purpose of this diagnostics device is not to transport FEL radiation to users, but exclusively to tune the undulator to achieve lasing and to reach optimum FEL conditions.

With this instrument, the spectral and spatial properties of the spontaneous radiation of single or multiple undulator segments can be investigated. As a

secondary application, through the use of absorbers or a limited number of few pulses in a train, the FEL radiation can also be observed.

These spectrometers of SASE1 and SASE2 will cover the main energy ranges of these beamlines. In the case of SASE3, with its lower photon energy, the higher odd harmonics of the spontaneous (or FEL) radiation will be observed.

2.3 Tasks for the undulator commissioning spectrometer system

The undulator commissioning spectrometer system is designed to enable the following tasks:

1. Main purpose 1: Relative adjustment of undulator segments (gap and K-parameter adjustment). The system allows measurements of the photon energy of the spontaneous radiation of each undulator segment in order to calculate and adjust the K-parameters to an accuracy required for FEL operation.
2. Main purpose 2: Adjustment of the phase between undulator segments. Intensity optimization by adjustment of the phase shifters between two adjacent undulator segments
3. Observation of the monochromatized beam properties (profile, intensity).
4. Spectral measurements of spontaneous or FEL radiation (averaged) by scanning the electron energy (fast) or by changing the crystal orientation (wide range).
5. Trajectory adjustment: Spatial evaluation of the higher harmonics of the spontaneous radiation, which have a smaller divergence than the fundamental for beam alignment.

3 Requirements and interface definition

This chapter describes the the requirements and interface definition for the K-mono device. Section 3.1 is related to the physical requirements for the device. The interfaces to other workpackages are described in section 3.2 (requirements for the other workpackages) and section 3.3 (requirements from other WPs for the device).

3.1 Requirements for the device

The requirements for the K-mono device derive from the undulator commissioning strategy described in Chapter 4, “Design description”. The main basis for these calculations is the quadrupole kick method [2], which promises to be the fastest and most accurate solution. However, the requirements of the other methods are also taken into account.

3.1.1 Basic requirements

We are considering mainly SASE1 and SASE2 specifications. The SASE3 wavelength range must be covered by this spectrometer by observing higher harmonic radiation, as the fundamental of the soft X-ray spontaneous radiation will have a too large divergence for being transmitted through the 8 mm beampipe apertures in the undulator section.

3.1.2 Measurement accuracy

For FEL operation, it is not necessary to tune the absolute K value to a high accuracy, but all undulator segments must be tuned to the same K, so that the relative error in the produced wavelength is smaller than the Pierce parameter:

$$\frac{\Delta\lambda}{\lambda} \leq \rho$$

For our calculations, we presume that the biggest variation of K will be between different undulator segments, rather than within a single segment. So it is sufficient to measure and compare the K parameter between the segments (if a suspicious undulator segment shall be investigated in more detail, this would also be possible with precise energy scans).

Equation 1:

$$K = \sqrt{2}\sqrt{\gamma^2 \frac{\lambda}{\lambda_u} - 1 - \gamma^2 \Theta^2}$$

$$\gamma = \frac{E}{m_e c^2}$$; Θ= observation angle; λ_u= undulator period

K can be calculated from this equation, which implies that one knows the electron energy (ΔE/E better than 2 x 10^{-4}) and the observation angle (should be zero) with high accuracy. As we are mainly interested in the measurement of ΔK, the third method (quadrupole kick), which compares the radiation of two undulator segments produced with the same electron bunch, will not be sensitive to the absolute electron energy or observation angle and will be much less sensitive to jitter effects.

The error in K for a given error in λ can be calculated from

$$\Delta K = \left(\frac{\delta K}{\delta \lambda}\right)\Delta\lambda \qquad \text{with } \Delta\lambda \le \rho\lambda$$

Table 2: *Maximal ΔK/K for FEL operation at different wavelengths*

λ [Å]	**bandwidth [%]**	**ρ = BW/2**	**K**	**ΔK < ρ*(1+K²/2)/K**	**ΔK/K**
1	0.08	4 x 10^{-4}	3.3	7.8 x 10^{-4}	2.4 x 10^{-4}
4	0.18	9 x 10^{-4}	6.1	2.9 x 10^{-3}	4.7 x 10^{-4}
16	0.3	15 x 10^{-4}	6.8	5.3 x 10^{-3}	7.8 x 10^{-4}

3.1.3 Measurement range

To cover the full gap range of the undulators, the devices should be tunable in following ranges:

1 Photon energy range for SASE1 and SASE2:
3–25 keV (core range 5–18 keV)

2 Photon energy range for SASE3:
0.28–3 keV (core range 0.4–2 keV)

With a crystal monochromator, we can cover the SASE3 range by observing the higher harmonics. When keeping K constant, it is possible to adapt the photon energy to the optimal K-mono range by setting the appropriate electron energy (between 8.5 and 17.5 GeV). When changing from 10 to 17.5 GeV, the energy of the fundamental increases by a factor of ~ 3.

3.1.4 Geometry and mechanics

The geometry is calculated for a distance from the end of the undulator of approx. 250 m:

1 Acceptance angle (incident beam):
> 15 µrad (acceptance of Bragg reflections may be less)

2 Beam dimensions (width):
max. ca. 10–12 mm (single beam)

3 Two spatially separated beams in horizontal direction:
> 20–24 mm horizontal acceptance

4 Theta (observation angle):
The main purpose of this device is an observation of the fundamental and odd harmonics of spontaneous radiation. So Theta should be zero.
A misalignment in Theta will lead in the four-bounce case to a significant suppression of the harmonics and total intensity.

5 Stability over a measurement period (a few hours):
± 0.1 mm and ± 1 µrad

A larger acceptance would be advantageous for lower photon energy, but, due to the large distance to the undulators, the crystal size would become too

large. Also the beampipe aperture would not allow the transmission of a beam with more than 38 µrad divergence (full beam profile), as would be the case for the fundamental radiation at lower photon energy.

3.2 Requirements for other work packages

3.2.1 Machine Layout Coordination (MLC)

Contact persons: Winfried Decking and Torsten Limberg

For the single segment K-tuning and non-spatially resolved pairwise K-tuning, it is essential to know the relative electron energy with a high accuracy and reproducibility. The precision of the absolute energy measurement can be lower.

The electron energy $\Delta E/E$ (see Section 1.2, “Project plan”) must be known to better than 2×10^{-4}.

That means we have the same accuracy requirement for the following:

- Relative electron beam energy jitter:
  $< 2 \times 10^{-4}$
- Low energy chirp:
  $< 2 \times 10^{-4}$
- Electron energy measurement resolution:
  Relative / absolute; bunch / averaged
- Beam position jitter / pointing stability (angle jitter):
  Minimum requirement: 30 µm / 0.5 µrad
- Electron energy scan over ± 1.5% (or more) within 10s:
  For some applications (e.g. the “steepest slope” tuning method), we need a fast electron energy scan in order to acquire a spectrum.

3.2.2 Undulator Systems (WP71, Joachim Pflüger)

Quadrupole mover: The quadrupole kick method for K-determination will demand an angular kick of ca. 20 µrad (> 35 µrad for lower photon energy). This requirement is covered by the beam steering requirement: A steering of the SASE beam to hit the first beam steering element in the photon beam transport that is the first offset mirror on the order of 500 m away from the movers. Alignment tolerances are about 0.01 m at this distance, yielding a required kick of 20 µrad (see Section 3.2.1, “Machine Layout Coordination (MLC)”).

3.2.3 DAQ and Control Systems (WP76, Christopher Youngman)

DAQ

The following signals have to be acquired and processed:

- Charge-coupled device (CCD) signal or scientific complementary metal-oxide-semiconductor (sCMOS) sensor signal, including camera control; continuous frame rate > 20 Hz (area of interest selection for fast frame rate > 10 kHz should be foreseen, if possible).
- Photocurrent of diodes: fast, bunch-resolved signal.
  A 10-channel DAQ board with 125 M samples/s board is currently under development in WP76. It will be equipped with pulse-stretching filters and FPGA for pulse energy analysis.
- Photodiode in a slow averaging mode (pulse train averaging)

Control

All standard motion control and some slow sensor control will be done by means of a Beckhoff control system:

- Retraction motion: stepper motor, movement range 75 mm , LVDT encoder (absolute and analog)
- Two rotary stages for crystal rotations (stepper motor; optical encoder): movement range 60°, resolution and repeatability better than 1µrad
- Height adjustment and chamber tilt: two stepper motors and a LVDT encoder

- Filter/attenuator control: stepper motor, five or more positions
- Detector movement for retraction and positioning of > 3 detectors, y-movement of 75 mm, resolution/repeatability better than 5 µm

Important

For all commissioning scenarios, we need (if possible direct) control over the following parameters and devices in a commissioning mode of the machine:

- Undulator gap movement:
  The most demanding case is gap scanning, where we would measure on the fly (i.e. during the continuous movement of the undulator gap). So, for each pulse train, the actual encoder value should be provided.
- Intersections in undulators:
  Quadrupole movers, air coils, and phase shifters have to be controlled for different measurement scenarios.
- Electron beam properties (e-beam energy, bunch compression)
- Apertures in front of the K-mono (e.g. the spontaneous radiation apertures (SRAs))
- 2D imager station behind the K-mono

In a safe commissioning mode, the number of bunches in a train would be limited to e.g. 300 pulses with two undulator segments. When all undulator segments are inserted, which in principle would make lasing possible, only single pulses would be allowed for a safe operation with the K-mono. Details have to be clarified during the development and definition of the equipment protection system (EPS).

3.2.4 X-Ray Optics and Beam Transport (WP73, Harald Sinn)

A beam collimator is a mandatory device before the K-mono. In any case, the beam collimation must allow a horizontal acceptance angle of ~ 35 µrad (from the first undulator segment). Vertically, the acceptance should be at least half of the horizontal acceptance (18 µrad).

It has to be checked whether the attenuator system for the K-mono (different from the beamline attenuator in XTD9) is part of the device, or if it can be

supplied by WP73. The required attenuation is on the order of 1000, to cover the range of spontaneous radiation from only one up to all segments, and higher if used for the FEL.

3.2.5 Survey and Alignment (WP32, Johannes Prenting)

Alignment to the theoretical beam axis:

Absolute accuracy: ± 0.3 mm and ± 100 µrad

As it is not planned to have remote control for a large alignment range; this level of accuracy has to be achieved during the installation and initial setup.

A manual coarse adjustment will be integrated into the support frame for all relevant degrees of freedom. A set of fiducial marks will be mounted at the chamber or the top plate of the adjustment stage.

3.3 Requirements from other work packages

3.3.1 X-Ray Optics and Beam Transport (WP73, Harald Sinn)

Vacuum requirements: strict requirements on outgassing and cleanliness come from the X-ray optics, as these use very contamination-sensitive devices.

As two of the K-monos could be very close to the first offset mirrors within a “particle-free” and hydrocarbon-free area of the beamline, there are stringent requirements to the design of the in-vacuum mechanical system [11].

3.3.2 Undulator Systems (WP71, Joachim Pflüger)

For air conditioning in the tunnels, the heat production is relevant.

Heat will be produced from motors outside the vacuum chamber and from electronics:

1 Heat load not connected to water cooling:
200 W (estimation of maximal load)

2 Heat load connected to water cooling:
< 2 kW (electronics rack, in-vacuum motors, photon beam absorption)

The physical requirements for the K-determination, in order to commission the undulators, are given in Section 3.1, “Requirements for the device”.

3.3.3 DAQ and Control Systems (WP76, Chris Youngman)

The compatibility and integratability into the European XFEL control system must be and were checked for all components within the K-mono, in collaboration with WP76. In particular, this was confirmed for the stepper motors, the encoders, their controllers, the digital and analog I/O, and the cameras.

3.4 Commissioning strategy

3.4.1 Central beam

For the determination of K, it is mandatory to find the central beam (i.e. to determine the zero position of observation angle Θ in Equation 1 on page 12).

By means of evaluating the centroid of the beam for each undulator segment, it is possible to correct the measurements for pointing errors. Besides the camera, a position-sensitive device like a four-quadrant diode or a diamond detector could also be used as a much faster option.

3.4.2 K- and ΔK-determination

Three different methods for K/gap-determination are taken into account (for details, refer to the cited papers). The first two methods require only an integral intensity measurement with a photodiode, so especially single segment tuning will be a fallback solution to the preferred quadrupole kick method, which requires a sensitive imager.

3.4.3 Single segment tuning and gap tuning

The energy spectrum of one undulator segment is measured (by switching off the others), in order to determine its effective K-value, which then has to be

adjusted by changing the gap accordingly. For this method, an integral intensity measurement with a sensitive photodiode is sufficient. With several thousand photons per single pulse, the diode signal should be big enough to measure individual pulses. The photon energy can be scanned by scanning the electron energy or the monochromator, while keeping the gap fixed. Alternatively, the gap can be varied at fixed observation energy for maximizing the intensity [3].

At Linac Coherent Light Source (LCLS) at SLAC National Accelerator Laboratory in Menlo Park, California, single segment spectra are currently measured by scanning the electron energy in a range of ± 1% because the monochromator energy is fixed by design. Each measurement point is being correlated with an electron energy measurement and normalized with an intensity measurement. In practice, some hundred pulses are necessary to measure one spectrum (Si111, four-bounce geometry at 8.13 keV).

3.4.4 Steepest slope

All but two adjacent undulator segments are “switched off” by opening the gap. Spectra of the fundamental (or a harmonic) are measured (by variation of E_e; electron energy scan and detection as in the first method) for different gap settings of one segment, while the other segment is kept at constant gap. For the setting with the steepest slope of the high energy edge, the K-parameters match best [1].

This method was developed at LCLS, but is currently not in use due to high noise.

3.4.5 Quadrupole kick

Also here, only the radiation of two adjacent undulator segments is examined. Between the segments, a quadrupole kick deflects the electron beam by up to 20 µrad. So the intensity profiles of the two segments, which originate from the same electron bunch, are spatially separated and can be directly compared. When observing the radiation produced by just one electron bunch, the electron energy jitter effect disappears. Due to the low intensity, a sensitive detector (e.g. an X-ray CCD) would be mandatory for single-shot measurements [2]. To avoid expensive detectors, we will use sensitive

standard equipment and average the signal from few pulses (10–100) taken from the same pulse train.

As it can be expected that the electron energy jitter within one bunch train is smaller than that between bunches of different trains, it would be possible to average up to 2700 pulses of one pulse train with a high signal-to-noise ratio. Furthermore, the requirements to DAQ would be quite relaxed (10 Hz frame rate). However, this integrating mode implies availability of long bunch trains of spontaneous radiation during undulator commissioning.

Nevertheless, when averaging bunches of different bunch trains with larger jitter effects, both undulator segments are affected equally. Energy chirp or jitter would broaden the averaged peaks, but, as long as the center of the peak can be determined with sufficient high accuracy, the relative K-measurement would not deteriorate.

In the initial accelerator commissioning phase, possibly only single bunches with 1 nC at 10 Hz are available (day-one scenario). An intensity calculation for this scenario is described in more detail below.

3.4.6 Scenario for day one

At day one, we have to take into account having only single bunches with 1 nC at a repetition rate of 10 Hz. So, in the case that the intensity from one pulse is not sufficient and averaging over seconds is necessary, there are higher requirements for the e-beam and detection stability. The camera, for example, must have a much lower dark current or readout noise. For this, we will use a 2.1 megapixel sCMOS camera from Photonic Science Ltd with a readout noise of 1.2 electrons and a dark current of 0.05 electrons per pixel per second.

On the other hand, it can be expected that the first undulator commissioning will be made at photon energies equal to or below 12.4 keV, so that all measurements can be performed using the Si 111 reflection. For an increase of energy resolution and a harmonics rejection, the four-bounce mode can be used.

One-bunch intensity (X-ray photons)

Parameters for calculations:

- E_e = 14 GeV (E_e = 10 GeV)
- E_{Ph}= 12.4 keV (E_{Ph}= 3 keV)
- Distance to first undulator segment = 450 m
- Distance to last undulator segment = 250 m
- Bunch charge = 1 nC
- Observation energy ~ 3 ‰ below fundamental or harmonic

Calculations of the peak intensity by Gianluca Geloni (WP72):

1 E_e = 14 GeV / E_{Ph}= 12.4 keV

Number of X-ray photons per mm² per bunch after the monochromator:

Distance from source (active undulator segment) to K-mono	**Si(111)**	**Si(333)**
Distance = 250 m	4 x 10^5	2 x 10^4
Distance = 450 m	1.2 x 10^5	6 x 10^3

2 E_e = 10 GeV / E_{Ph}= 3 keV / E_{obs}= 9 keV (third harmonic)

Number of X-ray photons per bunch after the monochromator per mm²:

	Si(111)	**Si(333)**
Distance = 250 m	1.6 x 10^5	8 x 10^3
Distance = 450 m	4.9 x 10^4	2.5 x 10^3

(One or two-bounce bandwidth used)

Detector efficiency / SNR, yield, and timing

It would be desirable if each X-ray photon on the screen could be detected (i.e. with a detection efficiency of one). Furthermore, a large dynamic range would be helpful, but can also be increased by the use of attenuators, in order to detect the radiation from undulators at largely different positions.

1 YAG screen / lens / mirror / camera

With a yield of the YAG:Ce screen (Crytur Ltd.) of 35 Ph/keV (photon-energy), we will have 350 visible photons per 10 keV X-ray photon emitted into 4π within the scintillator crystal. As the index of refraction n_{YAG} = 1.833, there is a loss of intensity by a factor of 0.3 in our case. Therefore, the optical system must have a large acceptance angle of 45° (full angle of accepted light cone, NA = sin(22.5°) = 0.38) or even more, which would collect about 1% of the visible light from the screen[1] [13]. That means that, per X-ray photon, we will have 3.5 visible photons in the camera. So, with a low-noise camera, it should be possible to reach a detection efficiency close to one. Maybe the efficiency could be optimized using a Si_3N_4 membrane with a phosphor layer.

2 Scintillator on fiber optic / CCD

For low-intensity measurements (single bunch), a CCD directly coupled to a scintillator, maybe via fiber optic taper, can be used. This should be more sensitive than the above-mentioned setup, but an sCMOS sensor cannot be used in this case.

How many bunches do we need, in order to achieve the required accuracy with the K-measurement?

With the calculated one-bunch intensities and the detector efficiency estimations from above, we can calculate the detected X-ray photons per pixel.

For the pixel size on the scintillation screen, we have to consider two effects: On the one hand, we need small pixels for high spatial resolution. On the other hand, the pixels must be big enough to collect enough photons for a high signal-to-noise ratio (requirement: S/N > 10).

Gianluca Geloni (WP72) wrote Mathematica scripts for calculating upper and lower limits of the pixel size, depending on the number of averaged bunches, the distance to the undulator segment, and the monochromator bandwidth.

---

[1] The ratio of collected light to light emitted into 4π is approximately $\frac{1}{4}\sin^2\theta$, where θ is the half-angle of the light collection cone, in this example 22.5°.

Results for different scenarios are shown in Graphs 1 to 3. Both conditions are fulfilled in the shaded area of the graphs.

Graph 1 shows the situation when averaging over 20 bunches by using the Si333 reflection with a bandwidth of 1.5 x 10^{-5} (single crystal or one channel-cut crystal). In order to meet both conditions, the field of view (and with it the pixel size on the screen) has to be adapted to the distance to the undulator segment. When averaging 100 bunches, a pixel size between 12 and 19 µm would fulfil both conditions, and one could use a fixed optics.

For the calculations, the bandwidth of the crystal reflections is taken from a one- or two-bounce case. The energy bandwidth of the Si111 four-bounce reflection would be two times smaller than the Si111 case, which can be sufficient for avoiding the Si333 reflection.

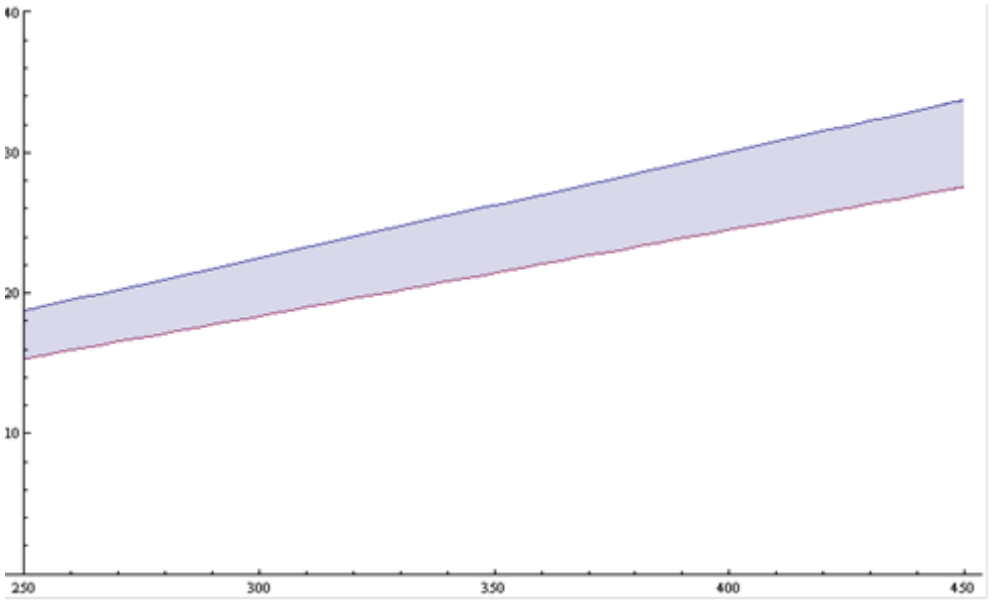

Graph 1: *Pixel size versus undulator distance – 20 bunches, Si333*

E_{ph} = 12.4 keV

E_e =14 GeV

Peak flux density in Nph/s/mm^2/0.1% BW (from SPECTRA simulation [14]):

Flux = 9.2 x 10^{10}

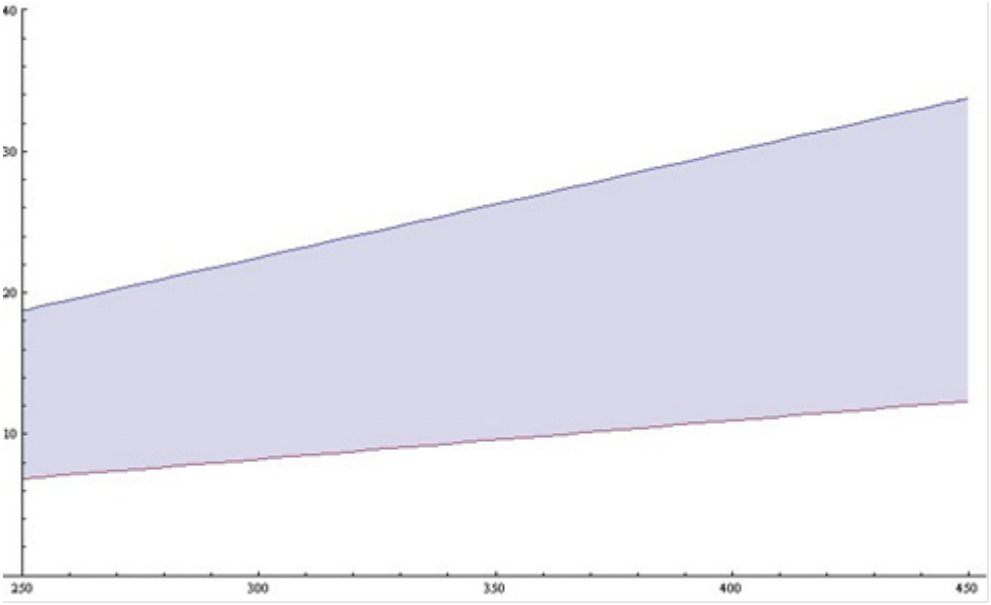

Graph 2: *Pixel size [µm] versus undulator distance [m] – 100 bunches, Si333*

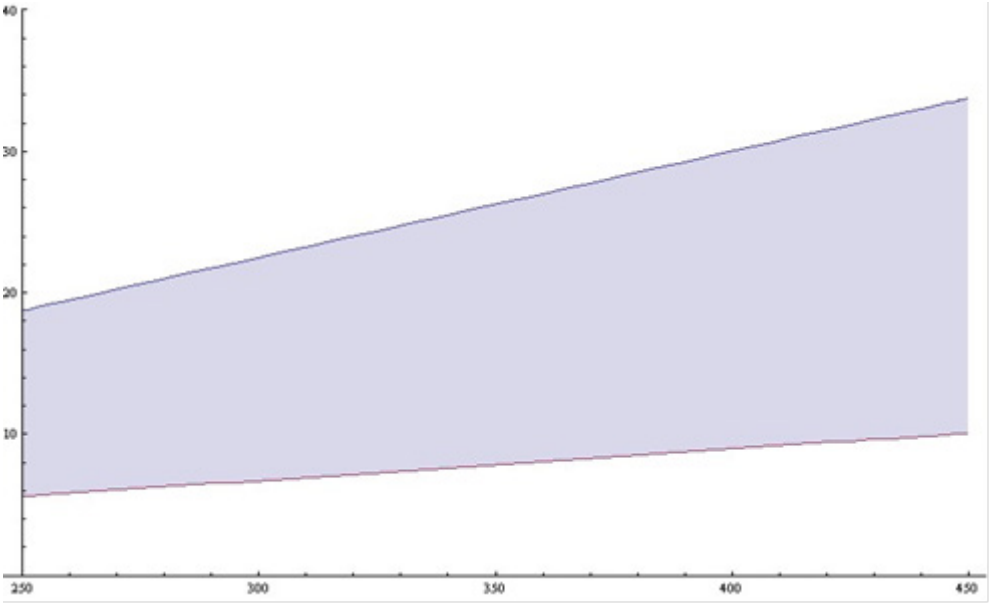

Graph 3: *Pixel size [µm] versus undulator distance [m] - 10 bunches, Si111*

3.4.7 Conclusion

Our calculations show that, at day one, we will also be able to use the quadrupole kick method, even when it has a high demand for the X-ray intensity. Using the Si 111 reflection, an acquisition of 10 to 100 bunches should be sufficient for one undulator segment measurement.

For the 333 reflection, long averaging time has to be taken into account, which could be a problem for acquiring gap curves with a large amount of data points.

In any case, we foresee an additional photodiode detector with which we can perform single segment tuning, as it is the current standard method at LCLS. This will also require the acquisition of several hundred data points per spectrum and will be in most cases slower.

3.5 Phase adjustment

The K-mono device can be utilized as a tool for phase adjustments of the undulator segments. The methods are not described in detail in this document, but two approaches are given here.

- When observing the photon flux at constant energy $E_{obs} = E_{fun}$ while changing the phase, the photon flux will vary by a factor of 700 for a phase advance from $\pi \rightarrow 2\pi$.
- Angular profile method (Tanaka):
  Close the gap of three adjacent segments and introduce a single kick between the second and third segment to separate the angular profiles. Vary the gap of the phase shifter between the first and second segment to look for maximum intensity, which can be normalized by the peak intensity corresponding to the third segment.

4 Design description

This chapter describes the design of the undulator commissioning spectrometer (K-mono) system. The requirements specified in chapter 3 were incorporated.

4.1 Introduction

Photon-based commissioning of the European XFEL undulators will require a precise adjustment of the K-parameters of all undulator segments and phasing between these segments. The LCLS approach, with a double channel-cut monochromator, was the basis for a conceptual design. For the SASE undulators at the European XFEL, we have to take into account the large gap setting range and wavelength ranges of 0.5–4 Å for SASE2 and 4–16 Å for SASE3, respectively. The spectrometer will analyse spontaneous radiation from single segments up to the full undulator length. In order to apply the spectrometer to the soft X-ray region of SASE3, the third, fifth, or even higher-order harmonics will be used.

4.2 Technical design

The technical design of the K-mono system is described here. The system consists of the main chamber with the double channel-cut monochromator, the filter chamber, and the detection chamber.

4.2.1 Monochromator setup

This section describes the general requirements and crystal stage setup for the monochromator part of the K-mono system.

General requirements

The K-mono device has the following general requirements:

- Physical requirements:
  See Chapter 3, “Requirements and interface definition”.
- Vacuum requirements:
  Experiences at LCLS show contamination of mirrors with carbon layers, which most likely comes from residual contamination with hydrocarbons in the vacuum system. So no outgassing of hydrocarbons, which would be cracked on sensitive optical surfaces, is allowed. That means metal vacuum seals should be preferred, and the use of vacuum grease (e.g. Krytox XHT-BDZ) will be limited to the most critical bearings. Dry lubrication will produce particles and is therefore not a real option.
- Compact design, due to space limitations in the tunnel

Crystal stage setup

- Channel-cut Si 111 crystal (see Figure 2)
- Indirect water cooling for temperature equalization
- Second monochromator stage for Bartels geometry with higher energy resolution and inline geometry. This allows slight detuning for suppression of harmonics.

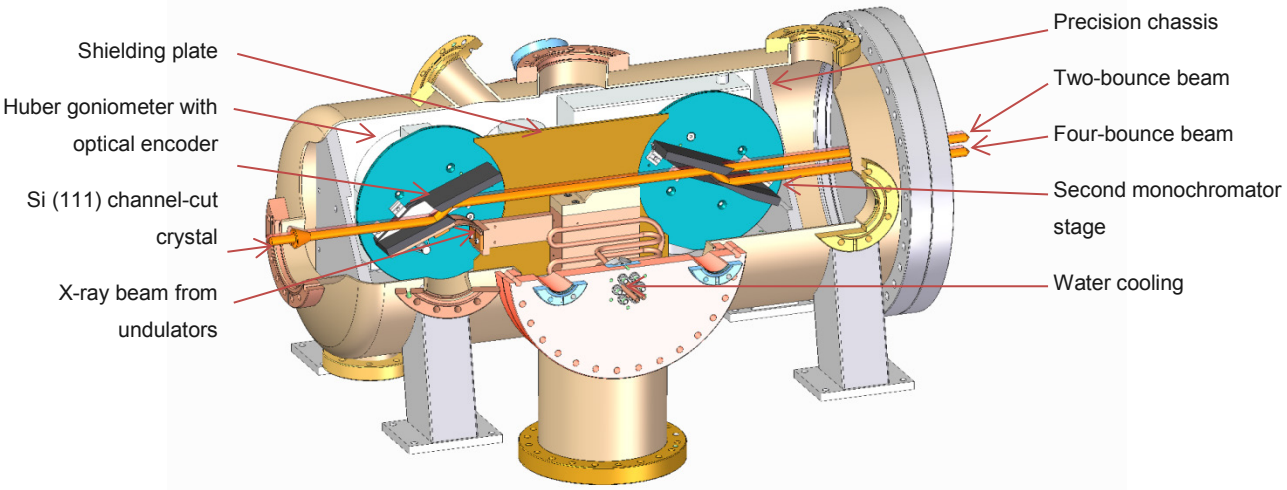

Figure 1: *Monochromator setup*

4.2.2 K-mono specifications

- Si channel cut crystals in two- and four-bounce geometry
- Bragg angle range: 7° to 55°
- Energy range: 2.5 keV to 16 keV for Si111 (7.5 to 48 keV for Si333)
- $\Delta E/E = 2 \times 10^{-4}$ for Si111 (1×10^{-5} for Si333)

Table 3: *Bragg reflections of Si 111 (symmetric reflections). Bragg angles in brackets are practically not useable because the required crystal size would be too large.*

	Bragg angle (°) **Acceptance angle (µrad)** **Energy resolution (eV)**		
Photon energy / eV	**Si111**	**Si333**	**Si444**
2400 / 5.2 Å	55.47° 187 µrad 0.30 eV	N/A	N/A
3100 / 4 Å	39.63° 105 µrad 0.42 eV	N/A	N/A
6200 / 2 Å	18.6° 46.5 µrad 0.90 eV	(73.08°) 31.5µrad 63 meV	N/A
12 400 / 1 Å	9.175° 21 µrad 1.77 eV	28.58° 5 µrad 0.12 eV	39.63° 5 µrad 75 meV
24 800 / 0.5 Å	(4.57°) 10.7 µrad 3.5 eV	13.84° 2.24 µrad 0.24 eV	18.6 ° 1.9 µrad 0.15 eV
40 000 / 0.31 Å	(2.83°) 6.6 µrad 5.74 eV	8.53° 1.36 µrad 0.39 eV	11.4° 1 µrad 0.23 eV

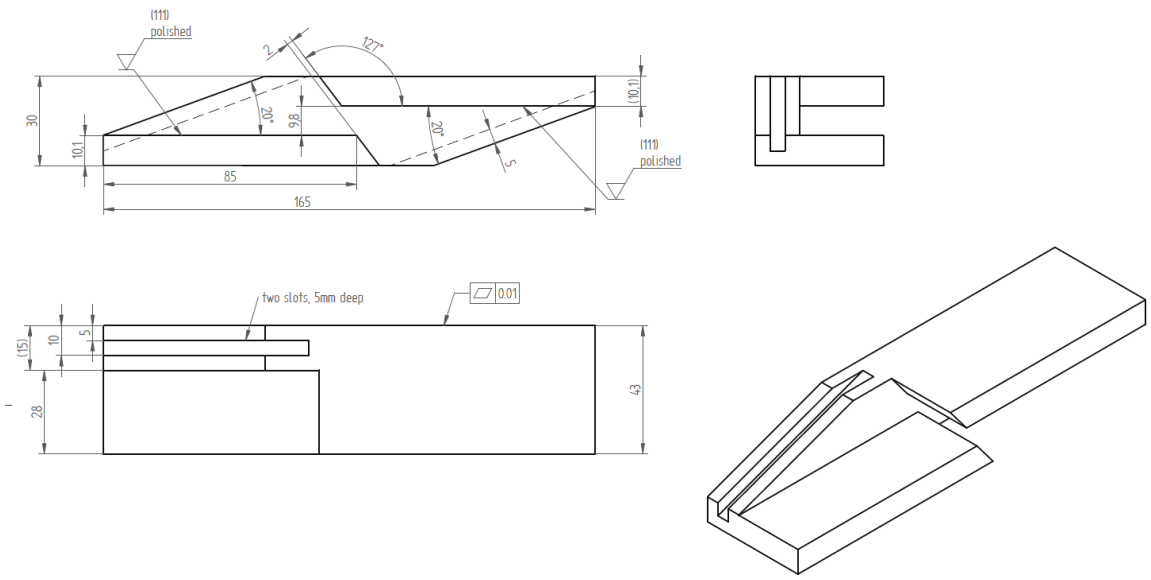

Figure 2: *Crystal drawing*

4.2.3 Rotation stages

The two rotation stages can be tuned individually. Furthermore, the second stage can rotate the second crystal pair out of the beam, in order to allow a 2-bounce operation of the monochromator.

From this and the physical requirements following main charachteristics must be implemented:

- Rotation repeatability accuracy better 1µrad
- Rotation range ~ 50° first stage, > 180° second stage
- First crystal holder with water cooling (indirect via copper braid) for temperature equalization

We have tested a UHV-compatible, high-precision rotary stage type 410D from HUBER Diffraktionstechnik GmbH & Co. KG with special vacuum grease Krytox XHT-BDZ (DuPont). The first setup has an incremental in-vacuum encoder (Renishaw TONiC) with one reference mark for homing. A second stage will be equipped with an absolute encoder (Renishaw RESOLUTE). This is not directly supported by a Beckhoff controller terminal, but an EtherCAT-compatible version is available by Elmo Motion Control Ltd (see Section 4.4, “DAQ and control hardware”).

4.2.4 Filter station

For energy calibration and diagnostics purposes, it will be necessary to bring filters or blockers for visible light into the beam. This filter shall be used together with the imagers and the K-mono for the spontaneous radiation (SR) beam; it is not foreseen to be used with the free-electron laser (FEL) beam. The position in the beamline is between electron beam separation and transmissive imager.

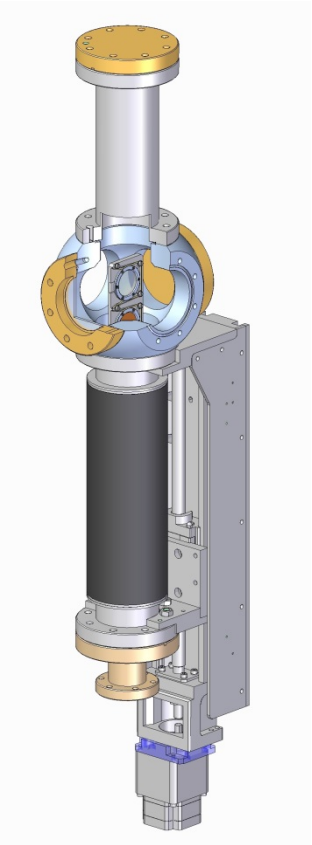

Figure 3: *Filter chamber*

Requirements:

- Large aperture – min. 28 mm x 10 mm
- Not only low-z materials
- No or only passive cooling
- Five different filter positions
- Full 40 mm ID aperture when fully retracted

- Optional shielding for misdirected FEL beam (aluminium or B4C plate)

This system will mainly consist of a small vacuum chamber, equipped with one linear manipulator. Spare flanges for viewports and electrical feedthroughs are also foreseen. At a later stage, the system could be upgraded with a load-lock. The filter holder is already designed to accommodate such an upgrade.

Filter materials for different energy ranges:

- Silicon or aluminium as low-z attenuators:
  Silicon has an absorption edge at 1839 eV
- Nickel foil:
  Absorption edge at 8333 eV
- Copper:
  8979 eV
- Chromium:
  5989 eV
- Molybdenum:
  20 000 eV
- At 17 038 eV:
  K-edge of Yttrium in the YAG screen (higher absorption leads to brighter a image above the K-edge)

4.2.5 Detection

All detectors will be vertically movable in order to allow the detection of the direct beam and inline beam in four-bounce geometry, as well as the parallel offset beam of the two-bounce case.

To be able to increase the energy resolution in case of the two-bounce setup, a movable and adjustable exit slit could be added:

- Retractable screen and/or detector
- Screen and CCD (or sCMOS / EMCCD) for imaging high or time integrated intensity
  - Pixel resolution between 10 and 20 µm (on screen)

- FOV > 25 mm horizontally x 12 mm vertically
- Low noise sensor for low intensity (spontaneous radiation of single undulator segment)
- Large dynamic range (for FEL)
- Scintillator screen (e.g. YAG:Ce)
- Optical system: e.g. taper or tandem lens with mirror [13]
  Camera must be protected from radiation (e.g. with mirror or lead glass disc)

- Diode detector for integral measurements:
  As an integral detector, we foresee a fully depleted photodiode with a thickness of 300 µm (e.g. Hamamatsu S3590-09):
  - Large enough to accept full spot (~ 10 mm)
  - Fast: single-shot capability
  - Should also accept third harmonic
- Option: Direct imaging X-ray CCD for low intensity and single bunch imaging. Sensitive and expensive device—not included in the initial setup. It will be checked whether the detection chamber can be designed in order to accept an X-ray CCD.

Even when it is planned to have some detection inside the monochromator chamber, an additional imaging detection chamber is planned (2D SR imager). This chamber will be adapted to the special geometrical requirements of the detectors. It will allow a shorter distance between scintillator screen and camera as well as observing the direct beam. Figure 4 shows a concept for an imager with high numerical aperture.

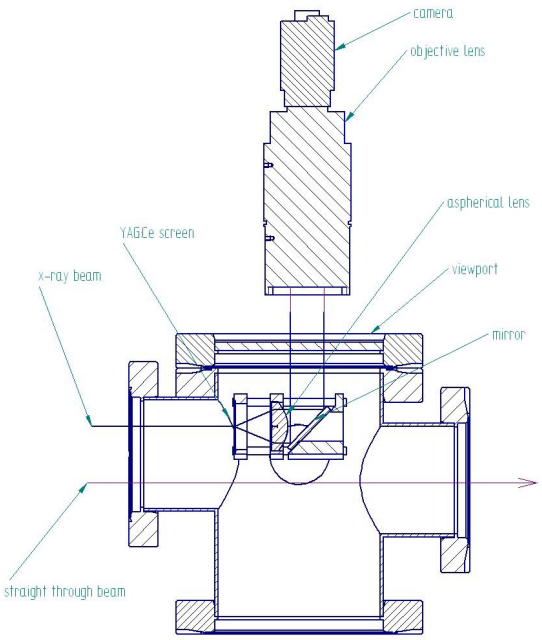

Figure 4: *Imager concept*

4.2.6 Retraction mechanism and adjustment stage

As the K-mono is not an online device, it has to be fully retractable from the direct beam. The detectors have to be movable for the two-bounce case (max. 20 mm), and their movement will be included in the detector chamber design. Following retraction mechanism is implemented:

1 The whole chamber is moved on a linear bearing outside the vacuum. Here, the detectors inside the K-mono chamber cannot be used in the direct beam (the monochromator can keep the wavelength adjustment).

2 The second channel-cut crystal can be rotated on the second goniometer stage out of the beam, in order to allow two-bounce operation.

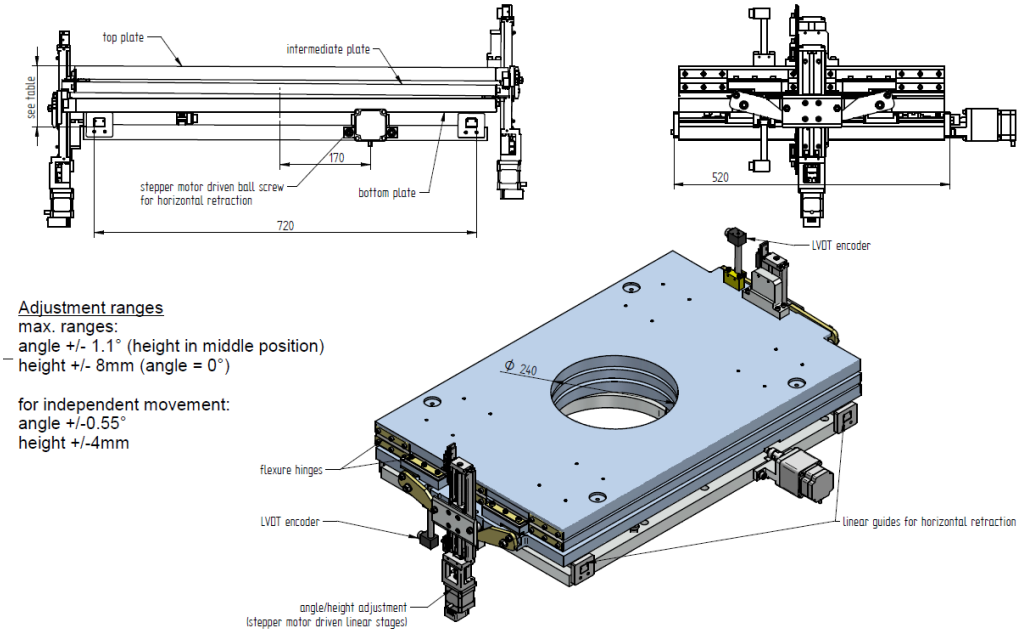

Figure 5: *Adjustment stage*

4.2.7 Position in the beamline

The position of the K-mono devices, including the SR part of the 2D imager, has shifted to upstream of the gas-based devices. For these devices and the differential pumping, it would be advantageous to decrease the apertures to a size that would be too small for the divergence of the spontaneous radiation that is observed by the K-mono.

The current positions are taken from the component list of the X-Ray Optics and Beam Transport group (WP73), EDMS document no. D00000002629421 Rev: O Ver: 2.

SASE 1 (XTD2)

Position: XTD2 Room 12

CAD room	Func. label	Device	Source dist. /m	LA (Z) /m
XTD2	KMON.2634.T9	K-mono system	200.25	2634.0271

SASE 2 (XTD1)

Position: XTD1 Room 10

CAD room	Func. label	Device	Source dist. /m	LA (Z) /m
XTD1	KMON.2596.T6	K-mono system	200.25	2595.5985

SASE 3 (XTD4)

Position: in XTD10 Room 2

CAD room	Func. label	Device	Source dist. /m	LA (Z) /m
XTD10	KMON.3114.T10	K-mono system	194.35	3113.6886

The reserved beamline length for the K-mono systems, including the SR imager, is 3 m.

4.2.8 System setup

The beamline height at the end of the undulator tunnels in SASE 1 and SASE2 is 2.6 m. Furthermore, the beamline is very close to the tunnel wall, so that, below the beamline, there is the transition between floor and wall. In order to create a flat base at a reasonable height (1400 mm below the beam) for the bench, we construct a concrete pedestal, which will be large enough for the K-mono device and the 2D imager.

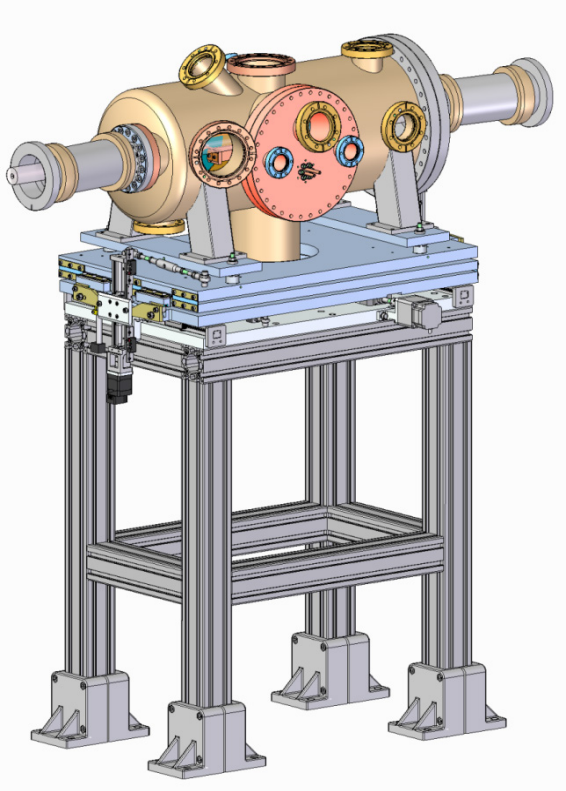

Figure 6: *K-mono device on its bench with the adjustment stage*

4.3 FEM simulations

For undulator commissioning, the requirements for mechanical stability and heat load are less stringent than if the beam had to be transported to the experiment hall. Nevertheless, a few points in the design were examined by means of finite element methods (FEM) analysis (ANSYS).

4.3.1 Crystal cooling

The cooling is intended to stabilize the temperature of the first crystal, as nearly all of the incoming spontaneous radiation power is absorbed on the first crystal surface. Lattice elongation due to heat load cannot be compensated with this fixed geometry of the channel-cut crystal. When the temperature difference is greater than ~ 5 K, the second Bragg reflection runs out of the rocking curve of the first crystal surface, and the monochromator

transmission decreases. The same is true for the second channel-cut crystal, but here the Bragg angle shift can be compensated.

Scenario for the SPECTRA simulation

An estimation for the heat load on the crystal was calculated with the synchrotron radiation calculation code SPECTRA [14].
With following assumptions, the spontaneous radiation power on the crystal is approximately 5 W :

- Two adjacent undulator segments
- 8 keV fundamental at 17.5 GeV electron beam
- 400 electron bunches (1 nC) per bunch train

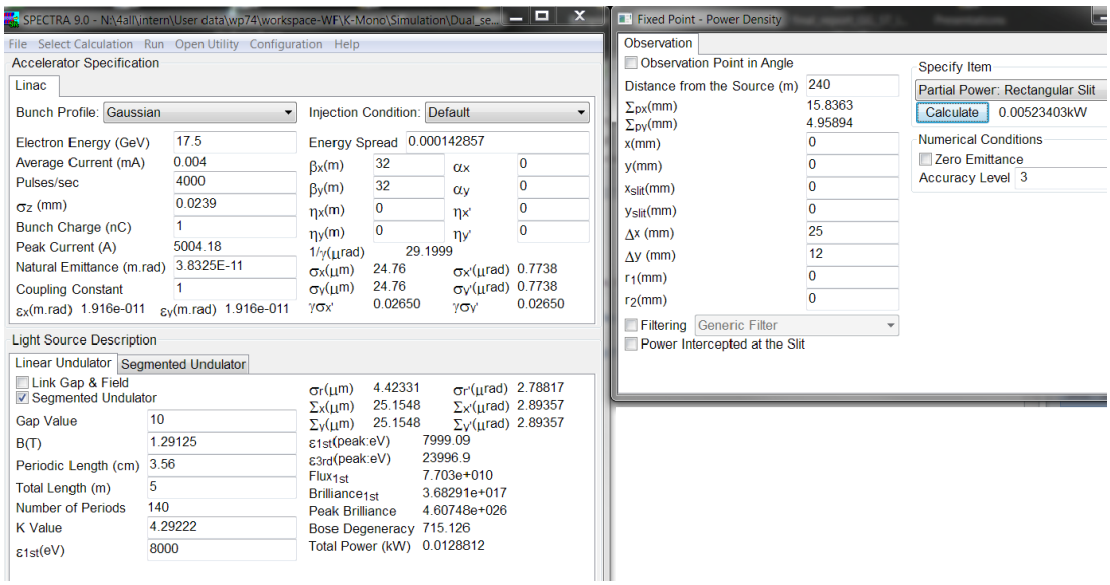

Figure 7: *SPECTRA simulation settings*

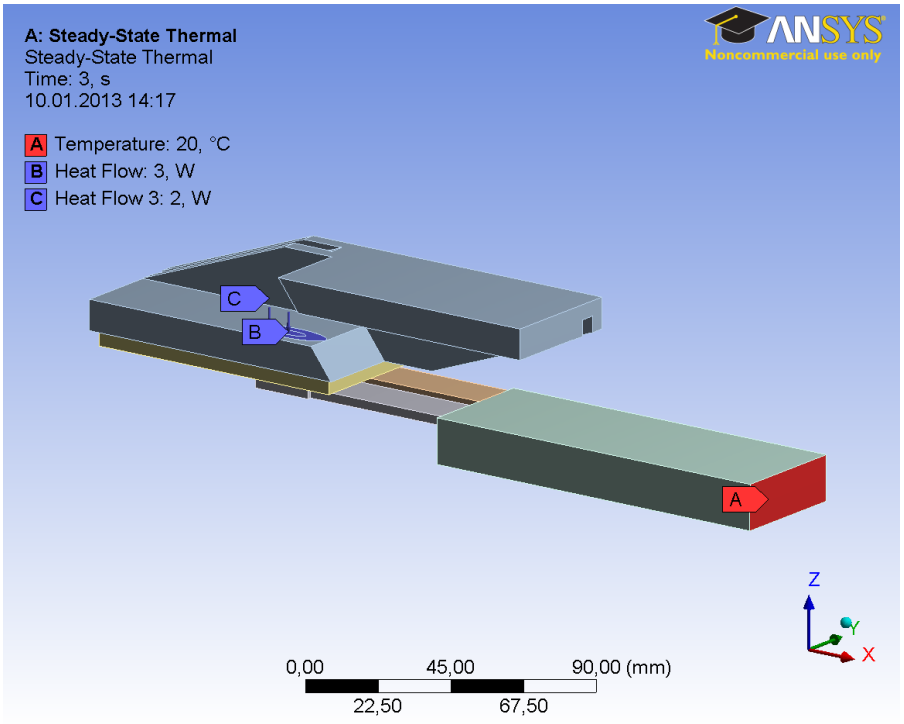

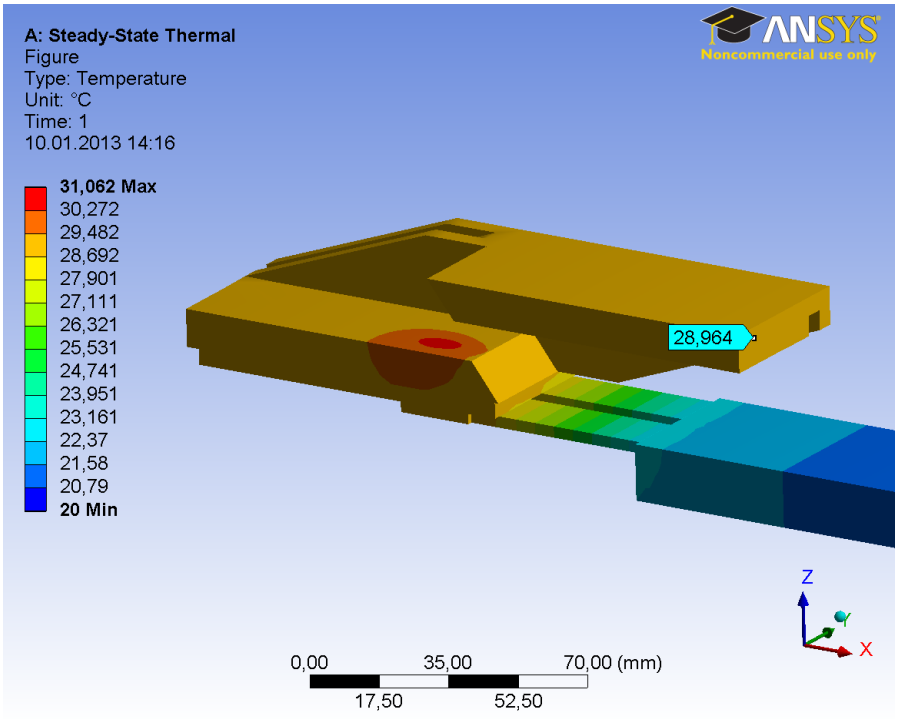

Figure 8: *Steady-state thermal simulation FEM results*

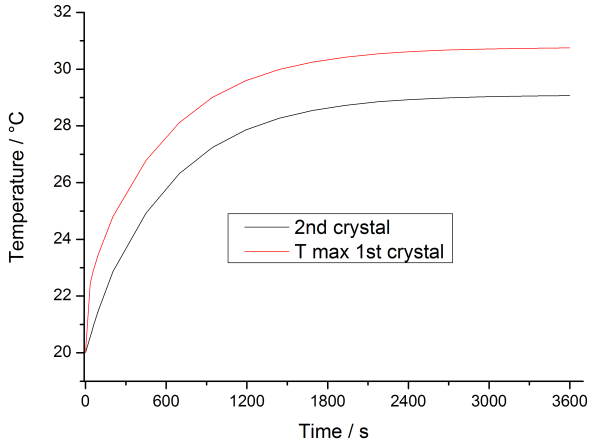

Figure 9: *Temporal temperature development of the first channel-cut crystal*

The temporal temperature development taken from the transient thermal simulation shows a temperature difference of less than 2 K between the two crystal surfaces of the first channel-cut crystal. For an estimation of the influence of the base plate as a heat reservoir, a few simulations with different plate parameters were performed. No big influence on the temperature difference was observed, just the time constant for the temperature rise increased.

Bragg angle correction of the first crystal stage:

On the second monochromator stage, the heat load is negligible and the Bragg angle shift of the first monochromator stage, caused by the temperature rise, must be taken into account. Table 4 shows the Bragg angle shift for different photon energies and temperature differences.

Table 4: *Si(111) Bragg angle shift due to temperature rise*

E_{photon} / keV	**θ_{Bragg}**	**$\Delta\ \theta_{Bragg}$(2K) /µrad**	**$\Delta\ \theta_{Bragg}$(5K) /µrad**	**$\Delta\ \theta_{Bragg}$(10K) /µrad**
3	41.227°	4.504	11.260	22.519
8	14.308°	1.311	3.277	6.555
12.4	9.175°	0.830	2.075	4.151

Table 5: *SASE1 and SASE2 parameters for the simulation (U40, max. K = 3.9)*

E_{e-} /GeV	$E_{fundamental}$ /keV	Absorbed power /W	Si (111) Bragg angle / DW-width	Si (333) Bragg angle / DW-width
10.5	3	1	12.7° / 30.8 µrad (third harm.)	23.3° / 4 µrad (fifth harm.)
10.5	12	0.3	9.5° / 21.4 µrad	29.6° / 5.3 µrad
14	5.4	2.4	21.5° / 54.5 µrad	21.5° / 3.6 µrad (third harm.)
14	20	0.7	NA (5.7° / 13.3 µrad)	17.3° / 2.8 µrad
17.5	8.5	5.1	13.5° / 32.8 µrad	44.3° / 9.2 µrad
17.5	24	1.9	NA (4.7° / 11.1 µrad)	14.3° / 2.3 µrad

Table 6: *SASE 3 parameters for the simulation (U68, max. K=9)*

E_{e-} /GeV	$E_{fundamental}$ /keV	Absorbed power /W	Si (111) Bragg angle / DW-width
10.5	0.37	0.74	36.4° / 102 µrad (ninth harm.)
10.5	2	0.3	19.2° / 48 µrad (third harm.)
14	0.66	2	36.8° / 104 µrad (fifth harm.)
14	3	0.9	12.7° / 30.8 µrad (third harm.)
17.5	1	4.5	16.4° / 40.5 µrad (third harm.)
17.5	3	2.4	12.7° / 30.8 µrad (third harm.)

4.3.2 Mechanical parts

Some critical parts were analysed by means of static structural analysis:

- Adjustment lever
- Bearing surfaces for cam rollers
- Spring elements for the flexure hinges

As a result, some parts were geometrically optimized. For the bearing surfaces, it was found that inlays made from hardened tool steel can prevent wear and deformation of the material.

4.4 DAQ and control hardware

Regarding DAQ and control, we follow the general requirements of the DAQ and Control Systems group (WP76). All control hardware was chosen to be compatible with the EtherCAT bus system by Beckhoff. So mainly Beckhoff terminals are used for the control of motors, encoders, switches, and analog signals. The only exception is the Huber rotary stage with an absolute Renishaw RESOLUTE encoder, where no Beckhoff terminal is available. In this case, a controller from Elmo is used which has an EtherCAT interface and is Beckhoff certified. The components are described in Table 7 and Table 8.

Table 7: *Adjustment stage control hardware*

Component		Type	Controller	Interface
Stepper motor 1	Y1	Oriental PKP243D15B-SG18-L	Beckhoff 7031 / 7041	EtherCAT
Stepper motor 2	Y2	Oriental PKP243D15B-SG18-L	Beckhoff 7031 / 7041	EtherCAT
Stepper motor 3	X	Oriental PK264B2-T20	Beckhoff 7031 / 7041	EtherCAT
LVDT 1	Y1	a.b.j. SM260.24.1.ST	SM127	0–10 V analogue
LVDT 2	Y2	a.b.j. SM260.24.1.ST	SM127	0–10 V analogue
LVDT 3	X	a.b.j. SM260.100.1.GHS	SM127	0–10 V analogue
6 limit / position switches	x/y	Omron D2VW-5L2A-1M	Beckhoff digital I/O or stepper controller	EtherCAT
Safety switch	X	Omron D2VW-5L2A-1M	(Enable input of motor controller)	(EPS/MPS)

Table 8: *Monochromator stages control hardware*

Component		Type	Controller	Interface
Stepper motor 1	Theta 1	Phytron VSS57.200-2.5-UHV	Beckhoff 7041	EtherCAT
Stepper motor 2	Theta 2	Phytron VSS57.200-2.5-UHV	Elmo DCBel 5	EtherCAT
Encoder 1 (*)	Theta 1	Renishaw TONiC / 1 reference position	Beckhoff 5101	RS485
Encoder 2	Theta 2	Renishaw RESOLUTE	Elmo DCBel 5	BISS-C
Four thermocouple sensors	T	Type K	Beckhoff 3314	EtherCAT
Four limit / position switches	Theta1/2	Huber	Beckhoff digital I/O or stepper controller inp.	EtherCAT

4.4.1 Photodiode detector

A fast photodiode for direct detection of X-rays will be integrated into the 2D SR imager after the monochromator or optionally on a manipulator in the K-mono chamber:

- Hamamatsu photodiode S3590-09
- Fast charge or current amplifier (e.g. Cividec, Femto)
- µ-TCA crate with timing board and digitizer chain (~ 100 Msamples/s) (will use system similar to that used by WP76 for the APD detection of the scientific WPs)
- In case of a linear manipulator: stepper motor, controller, limit switches, end switch

4.4.2 Filter manipulator with chamber

The filter chamber is positioned ca. 20 m upstream of the K-mono device but shall be controlled from the same control crate as the K-mono device:

- Stepper motor Oriental PKP264D28A-SG10-L (or similar)
- Beckhoff 7041 or 7051 controller

- Temperature measurement (optional, Type K thermocouple)
- 6 position switches
- End switch for MPS (out of beam position)

5 Prototype tests

In May and June 2012, one prototype of the undulator commissioning spectrometer (K-mono) was built and tested during two beamtimes at DORIS/BW1 and PETRA P01.

The prototype was built up as a two-bounce version with imaging detection, consisting of a YAG:Ce screen with camera, and a photodiode detector:

- K-mono setup with one monochromator stage / 1 crystal
- Test in helium atmosphere
- Test of four-bounce operation by means of using the high heat load monochromator of the beamline

5.1 Crystal test at HZB BESSY II

The first channel-cut crystal was manufactured in the crystal lab from Deutsches Elektronen-Synchrotron (DESY) HASYLAB and was characterized during a beamtime at Helmholtz-Zentrum Berlin (HZB) BESSY II in February 2012.

Figure 10: *Si(111) channel-cut crystal*

Here only the channel-cut crystal itself was brought for characterization to BESSY II:

- Mapping of the crystal surface at the PTB beamline
- Rocking curve mapping at the KMC1 beamline

The crystal surface mapping showed some scratches on the surfaces. From the rocking curve mapping, it could be seen that there were no big crystal defects and that the general crystal quality was sufficiently good.

In order to increase the optical performance, it was decided to have the crystal repolished at Crystal Scientific Ltd. together with the rest of the crystals that were also ordered there. As a result, all crystals now have the same surface quality with a tangential slope error of less than 20 μradians and a surface roughness of less than 20 Å.

5.2 Test at DORIS III BW1

As a preparation for the beamtime at PETRA III, functional tests were performed at DORIS III:

- Rotary stage control, in-vacuum Huber goniometer with optical encoder and stepper motor
- Compact linear stage with stepper motor for change between scintillator and photodiode after chamber

For these tests, the DAQ and Control Systems group (WP76) set up a preliminary control system with a prerelease of the Karabo control software.

5.3 Test at PETRA III P01

For further details about this test, see *Proc. of SPIE* 8504 [9].

At the P01 beamline of PETRA III, different undulator commissioning methods were tested.

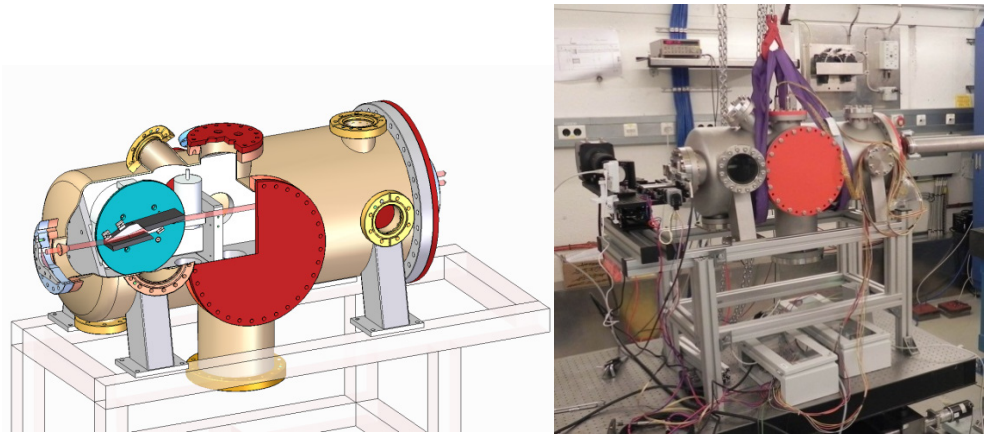

Figure 11: Left: *K-mono test setup (CAD).* Right: *Setup at PETRA III P01.*

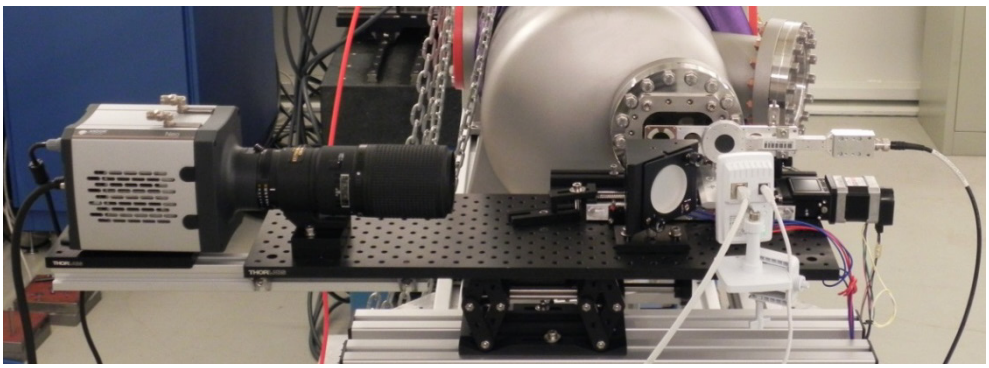

Figure 12: *Imager test setup at PETRA III*

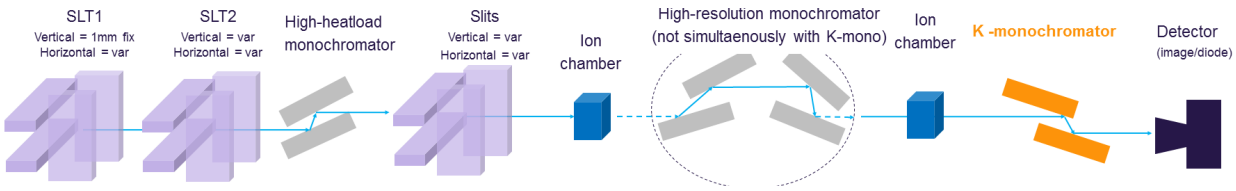

Figure 13: *Sketch of the experimental setup at P01. The high-resolution monochromator (HRM) was not used during the K-mono measurements. The HHM and the K-mono were set up to simulate the four-bounce case.*

5.3.1 Measurements

The following measurements were made at PETRA III P01 during a beamtime in July 2012:

1 Gap scanning with high-resolution monochromator (HRM):
Scanning the undulator gap of one undulator segment at a time and measuring the high-energy edge (with diode) at 14.4 keV

Aim: Reference measurement to obtain precision and check principle of K measurement method at a fixed energy.

2 Gap scanning with K-mono and HHM in four-bounce geometry (no HRM, only one undulator) at photon energies:
10, 11, 14.4 keV for Si(111)

- **a** Set undulator to the relevant K value required at the energy of interest. Take a reference spectrum
- **b** Set K-mono/HHM to an energy corresponding to a change in K of $1x10^{-4}$, $2x10^{-4}$ and $5x10^{-4}$
- **c** Scan gap for all different settings. See if an observable difference can be derived from the spectra, i.e. if relative K changes can be determined with the required precision.

Aim: Measure the resolution to which the K difference can be measured with the K-mono.

3 Imaging:
Set K-mono / HHM to an energy ~ 1% below the resonance.

Aim: Deduce K-parameter from transversal spatial distribution.

5.3.2 Results

Most importantly, the results of the gap scan spectra show that the resolution of the K-mono is good enough to measure the difference in K of two successive undulator segments with a sufficiently high accuracy (see Figure 14 on page 48 and Table 9 on page 49).

For the imaging technique, we could show that we could reproduce the spatial distribution of the SPECTRA simulation [14]. But as the HHM could not be removed from the beam, and as the beam aperture (maximal allowed slit size) was very small for the off-centre radiation, we could not quantify the beam properties from the picture. When using the K-mono in two-bounce operation for imaging, the SR-imager will be ~ 1 m from the crystal surface, so surface imperfections will not have a large influence on the picture.

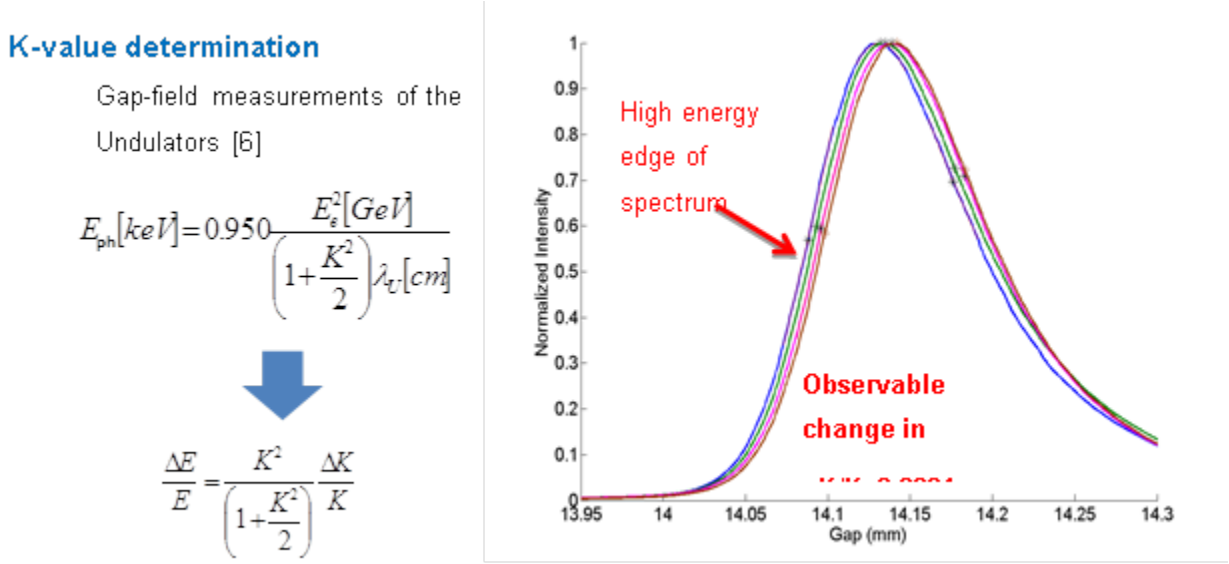

Figure 14: *Gap scan measurements*

Table 9: *Summary of the measurements and calculated K values from the scans at various energies*

U1 (fixed)	U2 (gap scan around; mm)	Monochromator set for energies (eV)	Centroid (Gaussian fit method)	K value	ΔK/K
Third harmonic of undulator for 14 400 eV; monochromator reflection Si(111)					
Open	14.13	14338.4	14.088	1.6108	Reference
		14339.8	14.093	1.6100	0.000497
		14341.7	14.096	1.6095	0.000807
		14346.6	14.098	1.6092	0.000993
Fundamental of undulator for 11 000 eV; monochromator reflection Si(111)					
Open	35.8	11005.5	36.84	0.16974	Reference
		11006.6	36.94	0.16809	0.0097
		11007.7	37	0.16712	0.0154
		11011.0	37.04	0.16648	0.0192

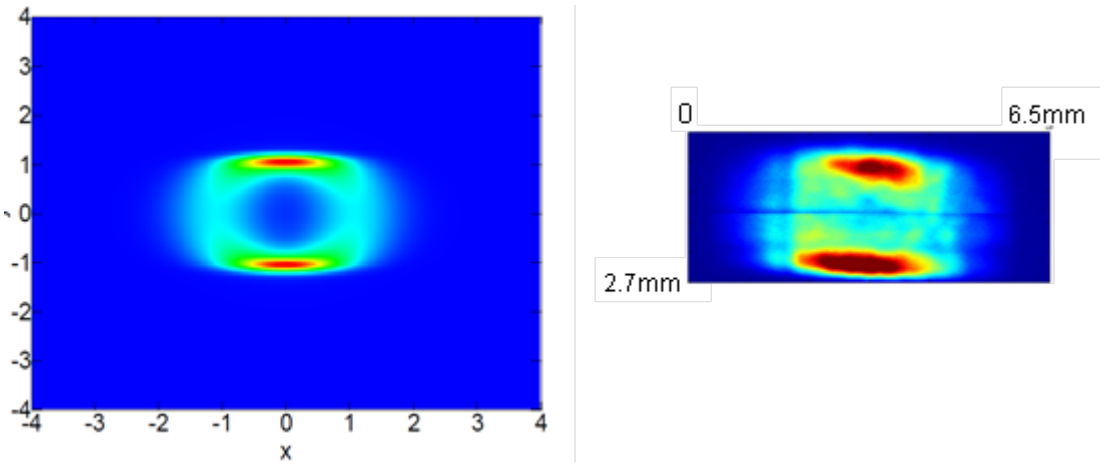

Figure 15: *SPECTRA simulation of SR of P01 undulator versus test images taken with the HHM, slightly detuned in energy (~ 1% below resonance). This test image is a composite image from two observations with different vertical positions of the high-heatload aperture of the beamline because this aperture is too small to allow recording a full-sized image at once.*

6 Safety analysis

6.1 General health and safety risks

6.1.1 Mechanical parts

(A) Moving parts

Moving parts can be:

- Linear translators (stepper or servo motor driven) e.g. for movement of adjustment stage, screen, camera, or detectors
- Linear actuators (pneumatic or magnetic) e.g. for filters
- Rotary stage of crystal main rotation
- Retraction of instrument from beam: movement of whole chamber

Unexpected movements of remotely controlled translators or actuators are usually not dangerous, as the movement range is small and the speed is slow. So no special protection is foreseen. The detailed construction will be assessed for possible danger to health or life because of unexpected movement of heavy parts. If necessary, protection against contact or a warning signal can be included.

(B) Special materials

For physical reasons, it might be unavoidable to use hazardous materials for:

- Shielding: lead bricks or plates outside the vacuum
- Heavy metal shielding parts must be marked according the standard regulations of the European XFEL Safety and Radiation Protection group
- Screens / detectors: scintillation materials
- Attenuators

The materials currently intended to be used in the system are mostly non-hazardous materials like YAG:Ce screens, nickel, and silicon.

Exception: Beryllium foil could be used as an attenuator. Beryllium and its compounds are highly toxic. Inhalation of the dust results in berylliosis, an inflammation of the lungs. These foils must be mounted in separate carriers (filter holder) and may not be machined.

When Beryllium is used as a blocker for optical light in the filter chamber, the chamber and the filter holder must be marked accordingly. The regulations of the European XFEL Safety and Radiation Protection group must be followed.

All materials are to be handled (at least for cleanliness reasons) with gloves and are never to be touched directly.

In any case, safety datasheets of the special materials used in the instrument should be included in the documentation.

6.1.2 Electronics

All electronics shall be built in compliance with CE safety requirements and RoHS. All cables have to be halogen free.

Possible use of hazardous voltages

Piezoelectric actuators can be supplied with voltages up to 200 V at low power. It is also possible that bias voltages at detectors can exceed 60 V. Appropriate cables will be used outside the vacuum (e.g. supplied by the manufacturer of the motor). Inside the chamber, the cables are Kapton or ceramic-insulated but might have open contacts. Only during tests or maintenance with an open chamber will there be access to non-insulated parts. So test setups with possible hazardous voltages will be protected by barriers.

6.2 Machine protection

Two potential critical situations for the machine are considered:

1. The free-electron laser (FEL) beam could hit some part of the system. Even the crystals, which are mainly designed for spontaneous radiation, could be damaged by a full FEL pulse train.
2. As the whole chamber is being moved for adjustment and retraction from the beam, a defective control system could potentially damage the bellows by driving the chamber beyond the end position.

In order to guarantee a clear aperture for FEL operation, a limit switch will signal the retraction position. An additional switch will be activated by a moving bar with the length of the maximal movement range. When this switch opens, the motor controller will be disabled. These switches will work independently from the control system and cannot be damaged by uncontrolled motor movements. If necessary, redundant switches can be mounted.

6.3 Special risks

6.3.1 Phase I: Prototype and initial tests

The usual rules for the buildup and testing of scientific instruments have to be followed. No further special risks have to be expected.

6.3.2 Phase II: Installation

The instruments for SASE1 and SASE2 will most likely be positioned in the undulator tunnels. Due to the space limitations there and the beamline height of 2.5 m, appropriate hoisting devices must be used. A working platform will also be necessary for installation (also maintenance) work at the instrument.

6.3.3 Phase III: Operation and maintenance

The instrument is placed in the undulator tunnel, shaft building, or the photon tunnel, which are equipped with an interlock system. So no additional risks

will appear during operation, as there is no access to the instrument, which then has to be operated exclusively by remote control.

In case of a beam shutdown, testing and maintenance would be possible, as the instrument in the tunnel would be accessible. A simple barrier could be used to avoid accidental touching of moving parts.

6.3.4 Phase IV: Decommissioning

Like other beampipe components, some mechanical parts of the instrument might get activated by the radiation. Therefore, proper disposal is possible only after measurements by the DESY radiation protection group (D3). In case of activation, the parts need to be handled according to the regulations of the D3 group.

In contrast to the mechanics, no activation has to be expected for the electronics. Since standard techniques are applied for production, standard disposal methods can also be used for the electronics boards.

List of figures

List of tables

References

[1] J. Welch et al.: "Undulator *K*-Parameter Measurements at LCLS", Proceedings of FEL 2009, Liverpool, UK (2009)

[2] T. Tanaka: "Undulator Commissioning Strategy for SPRING-8 XFEL", Proceedings of FEL2009, WEPC11, Liverpool, UK (2009)

[3] M. Tischer et al.: "Photon diagnostics for the X-ray FELs at TESLA", Nuclear Instruments and Methods in Physics Research **A** 483, 418–424 (2002) doi:10.1016/S0168-9002(02)00354-6

[4] J. Grünert: "Photon diagnostics requirements and challenges at the European XFEL" Proceedings of FEL 2009, MOPC56, Liverpool, UK (2009)

[5] T. Ishikawaa, K. Tamasakua, M. Yabashi: "High-resolution X-ray monochromators", Nuclear Instruments and Methods in Physics Research **A** 547 (2005) 42–49 doi:10.1016/j.nima.2005.05.010

[6] M. Altarelli et al. (ed): "The European X-Ray Free-Electron Laser: Technical Design Report", DESY Report 2006-097 (2006) ISBN: 978-3-935702-17-1 doi:10.3204/DESY_06-097

[7] T. Tschentscher, "Layout of the X-Ray Systems at the European XFEL", European XFEL Technical Report, XFEL.EU TR-2011-001 (2011) doi:10.3204/XFEL.EU/TR-2011-001

[8] H. Sinn et al.: "Conceptual Design Report: X-Ray Optics and Beam Transport", European XFEL Technical Report, XFEL.EU TR-2011-002 (2011) doi:10.3204/XFEL.EU/TR-2011-002

[9] C. Ozkan et al.: "Initial evaluation of the European XFEL undulator commissioning spectrometer with a single channel-cut crystal", Proc. of SPIE **8504**, 85040X (2012) doi:10.1117/12.929755

[10] J. Rehanek et al.: "Simulations of diagnostic spectrometers for the European XFEL using the ray-trace tool RAY", Proc. of SPIE **8141**, 814109 (2011) doi:10.1117/12.906038

[11] M.Dommach: "UHV Guidelines for X-Ray Beam Transport Systems", European XFEL Technical Note, XFEL.EU TN-2011-001-02

[12] X-ray Optics & Transport (WP73) Component list, EDMS Nr.: D00000002278111 Rev: C Ver: 2 Status: Released Dat.: 10 January 2013

[13] E.H. Ratzlaff, A. Grinvald: "A tandem-lens epifluorescence macroscope: Hundred-fold brightness advantage for wide-field imaging", Journal of Neuroscience Methods **36**, 127–137 (1991) doi:10.1016/0165-0270(91)90038-2

[14] T. Tanaka and H. Kitamura, J. Synchrotron Radiation 8 (2001) 1221

Acknowledgements

- Horst Schulte-Schrepping and Manfred Spiwek for providing the first prototype crystal
- DESY PETRA III:
  Hasan Yavas, Hans-Christian Wille, and the staff of P01 for the beamtime support
- DESY DORIS:
  Dimitri Novikov and Heiko Schulz-Ritter for the beamtime support
- HZB BESSY II:
  Jens Rehanek and Ivo Zizak
- X-Ray Photon Diagnostics group (WP74):
  Jan Grünert, Cigdem Ozkan (now at PSI), and Jens Buck
- Gianluca Geloni for intensity simulations and discussions, Sergey Tomin and Nikolay Smolyakov for simulations
- X-Ray Optics and Beam Transport group (WP73):
  Harald Sinn and his group members for a lot of help and discussions
- DAQ & Control Systems group (WP76):
  All members of the group for their constant support with the controls of the experiment setup